Ab initio Green's functions approach for homogeneous nuclear matter

F. Marino ⓘ *,^{a,*} **C. Barbieri** ⓘ *,^{b,c} **G. Colò** ⓘ *,^{b,c} **W. G. Jiang** ⓘ ^{a,d} **and S. J. Novario** ⓘ ^{e}

^{a}*Institut für Kernphysik and PRISMA+ Cluster of Excellence, Johannes Gutenberg-Universität Mainz, 55128 Mainz, Germany*

^{b}*Dipartimento di Fisica "Aldo Pontremoli", Università degli Studi di Milano, 20133 Milano, Italy*

^{c}*INFN, Sezione di Milano, 20133 Milano, Italy*

^{d}*Mainz Institute for Theoretical Physics, Johannes Gutenberg-Universität, 55128 Mainz, Germany*

^{e}*Department of Physics, Washington University in Saint Louis, Saint Louis, MO 63130, USA*

E-mail: frmarino@uni-mainz.de

Homogeneous nuclear matter is investigated using the *ab initio* Self-consistent Green's function approach with nuclear interactions based on chiral effective field theory. The employed method, which combines the state-of-the-art algebraic diagrammatic construction approximation at third order with Gorkov correlations, is capable of computing both the equation of state (EOS) and single-particle properties of nuclear matter. The EOS calculated with our approach and coupled-cluster theory are shown to agree very well. The one-nucleon spectral functions and the momentum distributions are discussed to gain insights into the dynamics of the interacting nuclear matter.

10th International Conference on Quarks and Nuclear Physics (QNP2024)
8-12 July, 2024
Barcelona, Spain

---

*Speaker

1. Introduction

Achieving a first-principle description of nuclear phenomena is a long-term endeavor of theoretical nuclear physics. At the most fundamental level, nucleons are bound states of quarks, and thus in principle nuclear physics could be described by quantum chromodynamics (QCD) in terms of quarks and gluons. However, at present, chiral effective field theory (χEFT) is the widely used framework for understanding nuclear interactions. χEFT describes nuclear forces consistently with the symmetries of the underlying theory of QCD, but in terms of the emergent degrees of freedom, i.e. nucleons and pions [1–4]. Advanced quantum-mechanical methods to solve the many-nucleon problem are the second, and equally crucial, pillar of the *ab initio* approach to nuclear theory [2–4]. Only the combination of both frameworks enables to provide first-principle predictions with controlled estimates of the theoretical error [3, 4].

In this contribution, a study of infinite nuclear matter with the Self-consistent Green's function (SCGF) many-body method [5–9] is presented. Nuclear matter is a homogeneous and extended system of interacting nucleons, which constitutes an essential model for neutron stars and a key microscopic input to astrophysical simulations [10, 11]. Therefore, it is crucial to be able to accurately predict nuclear matter properties. Also, the equation of state (EOS) (i.e, at zero-temperature, the energy per nucleon) is very sensitive to the low-energy constants on which chiral force models depend [12, 13].

In Sec. 2 we introduce the SCGF approach following [5, 7–9]. Predictions for the EOS in comparison with coupled-cluster theory [14, 15], the single-particle (s.p.) spectral functions (SF), and the momentum distributions are then reported in Sec. 3. Perspectives are outlined in Sec. 4.

2. Methods

In the SCGF method [5, 6, 16–18], the central object is the one-body (1B) Green's function (GF), which is determined by solving the Dyson or Gorkov equations, and whose knowledge allows to compute the total ground state (g.s.) energy and the g.s. expectation values of all 1B observables, While this approach is formally exact, the self-energy $\Sigma^{\star}(\omega)$ entering the Dyson equation must be approximated, in practice, by an expansion in terms of Feynman diagrams.

Our SCGF variant, see Refs. [7–9], is rooted in the Gorkov framework [16–18], and its key equation reads:

$$\left.\begin{pmatrix} T - \mu\mathbb{1} + \Sigma^{11}(\omega) & \Sigma^{12(\infty)} \\ (\Sigma^{12(\infty)})^{\dagger} & -(T - \mu\mathbb{1}) + \Sigma^{22}(\omega) \end{pmatrix}\right|_{\omega=\omega_q} \begin{pmatrix} \mathcal{U}^q \\ \mathcal{V}^q \end{pmatrix} = \hbar\omega_q \begin{pmatrix} \mathcal{U}^q \\ \mathcal{V}^q \end{pmatrix}. \tag{1}$$

The unknowns are the excitation energies $\hbar\omega_q$ and amplitudes $\mathcal{U}^q$, $\mathcal{V}^q$ (for each eigensolution q), which fully determine the GF $g^{11}(\omega)$. The chemical potential μ must be tuned for each fermion species to ensure the correct number of particles on average. Due to translational invariance, the GF of homogeneous matter is diagonal in the momentum basis and reads

$$g_{\alpha}^{11}(\omega) = \sum_{q} \frac{\left|\mathcal{V}_{\alpha}^{q}\right|^2}{\hbar\omega - \hbar\omega_q - i\eta} + \frac{\left|\mathcal{U}_{\alpha}^{q}\right|^2}{\hbar\omega + \hbar\omega_q + i\eta}, \tag{2}$$

with $\sum_q \left|\mathcal{V}_\alpha^q\right|^2 + \left|\mathcal{U}_\alpha^q\right|^2 = 1$. Here, α denotes the s.p. state with quantum numbers $\mathbf{k}_\alpha$ (momentum), t_α (isospin z-projection), and s_α (spin z-projection). The Gorkov GF is characterized by pairs of poles $\pm\hbar\omega_q$, which correspond to energies $\epsilon_q = \mu \pm \hbar\omega_q$ symmetric w.r.t. the chemical potential, and have weight $\left|\mathcal{V}_\alpha^q\right|^2$ ($\left|\mathcal{U}_\alpha^q\right|^2$) below (above) the Fermi surface μ. The momentum distribution ρ_α, which gives the occupation number for the state α in the interacting system, is readily obtained as $\rho_\alpha = \sum_q \left|\mathcal{V}_\alpha^q\right|^2$. Associated with the GF is the normal spectral function S^{11}, defined as

$$S_\alpha^{11}(\omega) = \sum_q \left[\left|\mathcal{V}_\alpha^q\right|^2 \delta(\hbar\omega + \hbar\omega_q) + \left|\mathcal{U}_\alpha^q\right|^2 \delta(\hbar\omega - \hbar\omega_q) \right]. \tag{3}$$

$$S(\mathbf{k}, \omega) = \sum_q \left[\left|\mathcal{V}_\mathbf{k}^q\right|^2 \delta(\hbar\omega + \hbar\omega_q) \right. \tag{4}$$

$$\left. + \left|\mathcal{U}_\mathbf{k}^q\right|^2 \delta(\hbar\omega - \hbar\omega_q) \right]. \tag{5}$$

In our scheme, most of the correlations are encoded in the normal self-energy $\Sigma^{11}(\omega)$, which is approximated using the state-of-the-art algebraic diagrammatic construction scheme [5, 17, 18] at third order [ADC(3)]. ADC is a powerful way of constructing an approximate self-energy that respects the analytical structure of the exact Σ^*, and automatically includes contributions to all orders in perturbation theory. Pairing correlations are taken care of by the anomalous component of self-energy $\Sigma^{12(\infty)}$, which here we approximate at first order [8, 9].

Coupled-cluster theory is also a diagrammatic post-Hartree-Fock (HF) expansion method [2, 14, 15]. The CC wave function has the form $|\Psi_0\rangle = e^T |\Phi_0\rangle$, with $|\Phi_0\rangle$ being a reference state. T, named cluster operator, is a superposition of n-particle-n-hole excitations. At the doubles level (CCD), T is truncated as $T \approx \frac{1}{4} \sum_{abij} t_{ij}^{ab} c_a^\dagger c_b^\dagger c_j c_i$, with the $2p2h$ amplitudes t_{ij}^{ab} determined by solving the CC equations. Accurate g.s. energies are obtained by adding perturbative triples ($3p3h$) corrections to CCD within the CCD(T) approximation [8, 14].

In addition, CC and ADC have been combined in the so-called ADC(3)-D schme [5, 8]. ADC(3)-D consists in inserting the CC amplitudes from a preliminary CCD calculation into the ADC coupling matrices, and its accuracy has been demonstrated in Ref. [8].

3. Results

We present results from the SCGF and CC methods with the ADC(3), ADC(3)-D, and CCD(T) truncations (Sec. 2) using the chiral ΔNNLO$_{go}$(450) interaction from Ref. [12]. Both CC and SCGF simulate the homogenous system using a cubic unit cell with a finite number of nucleons [8, 14, 19], Here, we use $N = 66$ neutrons in pure neutron matter (PNM) and $A = 132$ nucleons in symmetric nuclear matter (SNM) [19]. Periodic boundary conditions (PBCs) typically suffice to obtain the EOS. For s.p. properties, twist-averaged boundary conditions (TABCs) [9, 14], even though more demanding computationally, are preferred, as a denser mesh of k-points is obtained, thus allowing to better approximate the "true" infinite system.

The EOS of SNM (left) and PNM (right) are reported in Fig. 1. The inset shows the energies per particle, and an excellent agreement between the three sets of computations is found. The main

panels investigate the correlation energy per particle, and we can appreciate that predictions are very similar also on this scale. This confirms that these sophisticated many-body methods describe nuclear matter accurately [8]. Note also that the inclusion of CC-corrected coupling vertices in ADC(3)-D leads to very close agreement with CCD(T) [8].
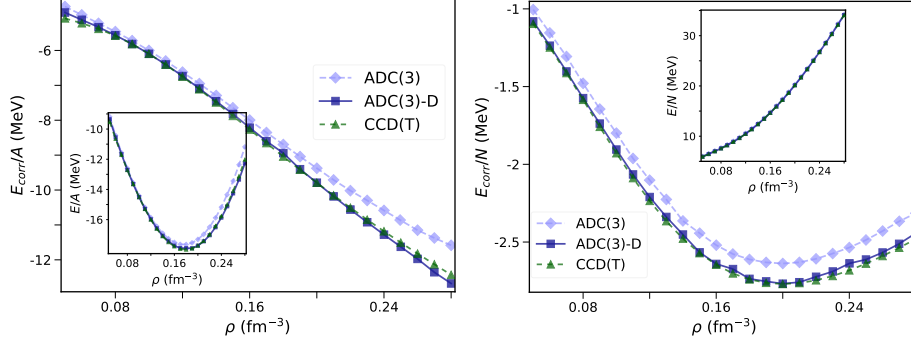

Figure 1: Correlation energy per particle (main panel) and energy per particle (inset) as a function of the number density in SNM (left) and PNM (right). Calculations have been performed with the ADC(3), ADC(3)-D and CCD(T) methods. The ΔNNLO$_{go}(450)$ interaction from Ref. [12] is employed, and PBCs are imposed.

In Fig. 2, the SF (3) is shown for SNM (left) and PNM (right). S^{11} is represented as a two-dimensional map as a function of the momentum $k = |\mathbf{k}_\alpha|$ (horizontal axis) and the energy $\hbar\omega$ (vertical axis). Poles ϵ_q are denoted by dots, and a color scale is used to represent the value of the strengths $\left|\mathcal{V}_\alpha^q\right|^2$ ($\left|\mathcal{U}_\alpha^q\right|^2$) for energies below (above) the Fermi level μ. The strong correlations that characterize SNM are manifest in the increased fragmentation of the SF at momenta $k > 1.5\,\mathrm{fm}^{-1}$. In both SNM and PNM, the dominant peaks, as well as HF energies (crosses), follow a roughly parabolic trend as a function of k, which is driven by the kinetic energy $\sim k^2$. The SNM spectrum is highly fragmented and shows a wealth of satellite peaks, especially for large k and $\hbar\omega$. In PNM, where correlations are weaker, the background is fainter and the primary branch dominates well into the high-momentum region. In both cases, states close to the Fermi momentum feature a single dominant pole with $\left|\mathcal{V}_\alpha^q\right|^2 \simeq 1$ for $k < k_F$ or $\left|\mathcal{U}_\alpha^q\right|^2 \simeq 1$ for $k > k_F$. Our *ab initio* calculations thus validate microscopically the picture of Landau quasi-particle excitations at the Fermi surface [20, 21].

Finally, momentum distributions $\rho(k)$ in SNM (left) and PNM (right) with both PBCs (circles) and TABCs (empty squares) are shown in Fig. 3. While in a HF picture states below (above) the Fermi momentum are completely occupied (empty), in the interacting system hole states ($k < k_F$) are partially depleted. The depletion is much larger in SNM, due to stronger correlations. Conversely, a momentum tail appears above k_F, with particle states being partially populated, while a finite discontinuity across the Fermi surface is preserved also in the presence of interactions.

4. Conclusions and perspectives

We have investigated infinite nuclear matter using the ADC-SCGF *ab initio* method. We have studied both the EOS, which agrees very well with coupled-cluster [8], and single-particle
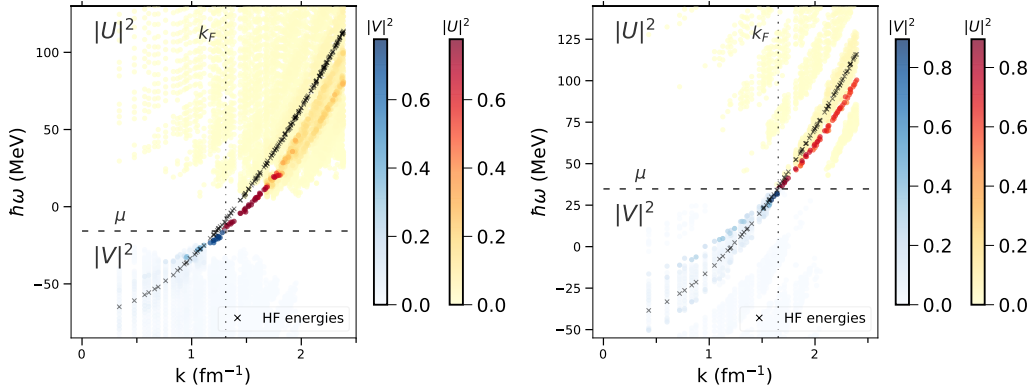
Figure 2: Two-dimensional representation of the spectral function for SNM (left) and PNM (right) as a function of the momentum k and the energy $\hbar\omega$. Calculations are performed at $\rho = 0.16\,\mathrm{fm}^{-3}$ with ADC(3) employing TABCs with the ΔNNLO$_{\mathrm{go}}(450)$ interaction. The Fermi momentum k_F and the chemical potential μ are marked by dotted and dashed lines. The squared amplitudes $\left|\mathcal{U}_\alpha^q\right|^2$ ($\left|\mathcal{V}_\alpha^q\right|^2$) are shown for poles above (below) the Fermi level. The color scale is shown next to each plot. HF s.p. energies are represented by crosses. For SNM, the neutron part of the SF is displayed.
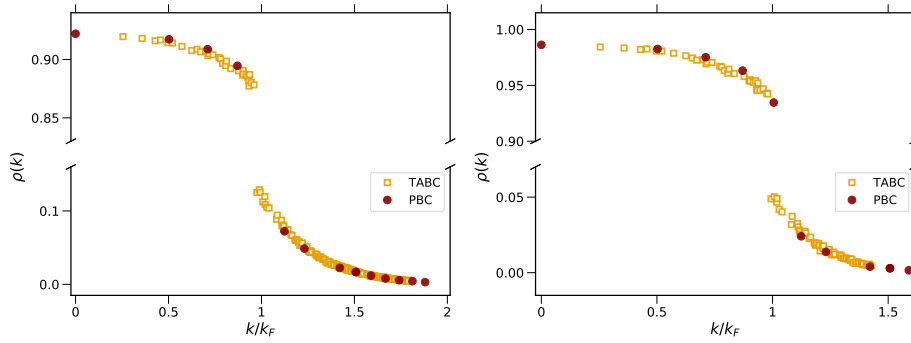

Figure 3: Momentum distributions $\rho(k)$ as a function of k/k_F for SNM (left) and PNM (right) at density $\rho = 0.16\,\mathrm{fm}^{-3}$. Calculations performed with ADC(3) with PBC (circles) and TABC (empty squares) are compared. Note that different scales are used on the vertical axis for points below and above the discontinuity.

properties. We plan to apply ADC to superfluid neutron matter, quasi-particle properties (effective mass, lifetimes), and momentum distributions across densities and isospin asymmetries.

References

[1] R. Machleidt and F. Sammarruca, *Chiral eft based nuclear forces: achievements and challenges*, *Physica Scripta* **91** (2016) 083007.

[2] M. Hjorth-Jensen, M.P. Lombardo and U. van Kolck, eds., *An advanced course in computational nuclear physics: Bridging the scales from quarks to neutron stars*, vol. 936 of *Lecture notes in physics*, Springer, Cham (2017), 10.1007/978-3-319-53336-0.

[3] H. Hergert, *A guided tour of ab initio nuclear many-body theory*, *Frontiers in Physics* **8** (2020) 379.

[4] A. Ekström, C. Forssén, G. Hagen, G.R. Jansen, W. Jiang and T. Papenbrock, *What is ab initio in nuclear theory?*, *Front. Phys.* **11** (2023) 1129094 [2212.11064].

[5] C. Barbieri and A. Carbone, *Self-consistent green's function approaches*, in *An Advanced Course in Computational Nuclear Physics: Bridging the Scales from Quarks to Neutron Stars*, M. Hjorth-Jensen, M.P. Lombardo and U. van Kolck, eds., (Cham), pp. 571–644, Springer International Publishing (2017), DOI.

[6] A. Rios, *Green's Function Techniques for Infinite Nuclear Systems*, *Front. in Phys.* **8** (2020) 387 [2006.10610].

[7] F. Marino, *Microscopic theory of infinite nuclear matter and non-empirical energy functionals*, Ph.D. thesis, Università degli Studi di Milano, 2023.

[8] F. Marino, W.G. Jiang and S.J. Novario, *Diagrammatic ab initio methods for infinite nuclear matter with modern chiral interactions*, *Phys. Rev. C* **110** (2024) 054322.

[9] F. Marino, C. Barbieri and G. Colò, *in preparation*, 2024.

[10] G. Burgio, H.-J. Schulze, I. Vidaña and J.-B. Wei, *Neutron stars and the nuclear equation of state*, *Progress in Particle and Nuclear Physics* **120** (2021) 103879.

[11] P. Haensel, A.Y. Potekhin and D.G. Yakovlev, *Neutron stars 1: Equation of state and structure*, vol. 326, Springer, New York, USA (2007), 10.1007/978-0-387-47301-7.

[12] W.G. Jiang, A. Ekström, C. Forssén, G. Hagen, G.R. Jansen and T. Papenbrock, *Accurate bulk properties of nuclei from $a = 2$ to ∞ from potentials with Δ isobars*, *Phys. Rev. C* **102** (2020) 054301.

[13] C. Drischler, J. Holt and C. Wellenhofer, *Chiral effective field theory and the high-density nuclear equation of state*, *Annual Review of Nuclear and Particle Science* **71** (2021) 403.

[14] G. Hagen, T. Papenbrock, A. Ekström, K.A. Wendt, G. Baardsen, S. Gandolfi et al., *Coupled-cluster calculations of nucleonic matter*, *Phys. Rev. C* **89** (2014) 014319.

[15] G. Hagen, T. Papenbrock, M. Hjorth-Jensen and D.J. Dean, *Coupled-cluster computations of atomic nuclei*, *Reports on Progress in Physics* **77** (2014) 096302.

[16] V. Somà, *Self-consistent green's function theory for atomic nuclei*, *Frontiers in Physics* **8** (2020) 340.

[17] V. Somà, T. Duguet and C. Barbieri, *Ab initio self-consistent gorkov-green's function calculations of semimagic nuclei: Formalism at second order with a two-nucleon interaction*, *Phys. Rev. C* **84** (2011) 064317.

[18] C. Barbieri, T. Duguet and V. Somà, *Gorkov algebraic diagrammatic construction formalism at third order*, *Phys. Rev. C* **105** (2022) 044330.

[19] F. Marino, G. Colò, X. Roca-Maza and E. Vigezzi, *Perturbed nuclear matter studied within density functional theory with a finite number of particles*, *Phys. Rev. C* **107** (2023) 044311.

[20] A. Rios and V. Somà, *Self-consistent green's function calculation of the nucleon mean free path*, *Phys. Rev. Lett.* **108** (2012) 012501.

[21] W.H. Dickhoff and D.V. Neck, *Many-Body Theory Exposed!*, World Scientific Publishing (2004).